Long Term Partial Discharge Behavior of protrusion defects in HVDC GIS

Cong Thanh Vu, Caterina Toigo, Frank Jacquier and **Alain Girodet**
SuperGrid Institute
23 rue Cyprian
69100 Villeurbanne France

Maximilian N. Tuczek
TenneT TSO GmbH
Bernecker Straße 70
95448 Bayreuth

Uwe Riechert
Hitachi Energy Switzerland
Brown-Boveri-Strasse 5
Zurich 8050, Switzerland

Armando Rodrigo Mor
Universitat Politècnica de València
Instituto de Tecnología Eléctrica
46022 Valencia, Spain

ABSTRACT

In this paper long term partial discharge (PD) behavior of protrusion defect in real size High Voltage Direct Current Gas Insulated Switchgear (HVDC GIS) is studied for SF_6 and SF_6 alternative gases including Fluoronitrile – CO2 mixture (10 %) and Fluoroketone – Dry Air mixture (6.6 %). The evolution of PD apparent charge and PD repetition rate for all investigated gases are presented and discussed. Measurement results point out that the PD behavior changes with time. The PD apparent charge increases and the PD repetition rate decreases generally with the increase of voltage application time. This evolution can be associated with the change of protrusion tip radius due to electrochemical etching: The tip radius of the protrusion being enlarged. Besides, the Pulse Sequence Analysis (PSA) plots of the PDs caused by this defect are also presented. It is observed that the PSA plots change also with time. For development of an effective PD monitoring and defect recognition tool and thus risk assessment in operation of HVDC GIS, it is necessary to take these changes into account.

Index Terms — partial discharge (PD), PSA, HVDC GIS, SF_6, SF_6 substitute, Fluoronitrile, Fluoroketone, defect recognition

1 INTRODUCTION

HIGH Voltage Direct Current (HVDC) is an interesting technology for energy transmission thanks to its very low losses. It is particularly adapted for transmission over long distances [1]. With the multiplication of renewable and offshore energy productions which are usually far away from the consumption sites, together with the development of power electronics, the HVDC technology becomes more and more important in the energy transmission topology.

The development of HVDC transmission requires the corresponding HVDC components including Overhead Lines (OHL), cables and substations. Among different technologies for substations, metal-enclosed Gas Insulated Switchgear (GIS) is a highly reliable technology that has advantages like the space saving and the immunity to environmental conditions. These characteristics make it very interesting to replace conventional substation, especially in offshore applications.

Partial discharge (PD) measurements are an important tool for testing the dielectric integrity. With the help of PD diagnostics, it is possible to confirm that no defects were introduced during production in the facture or during transport or assembly on side. Moreover, PD measurements can also be used as a diagnostic tool during operation of GIS to detect presence of defect and then to determine the risk of a dielectric breakdown. They can be then used in condition-based maintenance asset management strategies. PD in High Voltage Alternative Current (HVAC) GIS is well-studied and different tools are already employed in industrial applications for online monitoring. Nevertheless, in HVDC GIS, the study of PD behavior, the defect identification and recognition are less investigated and cannot be adopted directly from AC e.g. because at DC no synchronization with voltage phase is possible.

The GIS needs to be filled with insulating gas in order to ensure the insulation between the high voltage conductor and the grounded enclosure. The insulating gas is up to now usually

SF_6 which is an excellent dielectric gas, but it has the highest known greenhouse effect. The utilization of SF_6 gas is subjected to regulation [2] as it is listed in Kyoto protocol.

To reduce the environmental impact of SF_6 gas, alternative solutions to SF_6 were introduced these recent years into the AC market to prove their performances. Among different investigations, Novec 4710 - Fluoronitrile (C_4FN) and Novec 5110 -Fluoroketone (C_5FK) mixtures with buffer gas as CO_2 or Dry Air are identified as promising solutions for the HVAC GIS energy transmission assets [3]. The application of these gases could be then extended for HVDC transmission as well as for HVDC GIS.

It should however be underlined that the PD investigations in DC voltage are limited and even more for SF_6 alternative gases. According to our knowledge, there are some works which investigated the PD characteristics of different defects in DC voltage but often on small scale test setup and with conventional gases such as N_2, air, and SF_6 [4][5]. However, the results obtained from investigations on small scale test equipment might not be easily extrapolated to the full-size equipment due to the scale effect.

Concerning the PD behavior of defect in full-size equipment, some authors presented measurements of a protrusion defect in GIS under DC voltage for N_2, SF_6 and air gases in a real size GIS [6][7]. They showed PD behavior dependence on the gas pressure, on the voltage, and the type of gas. When the conventional gases like SF_6 or natural gases are replaced by the C_4FN – CO_2 mixture or C_5FK – Dry Air mixtures with equivalent dielectric strength, the PD characteristics of a protrusion defect were presented in [8]. It is observed that the higher PD apparent charge is obtained with negative polarity in SF_6 while the opposite tendency is obtained for C_4FN – CO_2 and C_5FK – Dry Air mixtures. This change of behavior is explained by the difference of PD behavior between SF_6 and the buffer gas meaning the CO_2 and Dry Air [8]. The polarity dependence of PD apparent charge observed in DC is in accordance with the results obtained in AC during the positive or negative half wave [9].

According to the authors' knowledge, there is up to now no study about long-term behavior of partial discharge in DC voltage at different gas mixtures. However, in DC voltage, physical phenomena can change with time due to the transition of the electric field from a capacitive distribution to resistive distribution, which can vary from days to months [10]. Moreover, the phenomena of charge accumulation on both surface and volume can strongly impact the electric field distribution. Furthermore, if the PD characteristics of the defect change with time, it can lead to some difficulties for the development of robust defect detection and recognition tools. In this case, the defect characterization should be studied at different stages. The findings are a decisive basis for defect recognition and thus risk assessment in operation. Therefore, the aim of this paper is to study the PD long-term behavior of not only SF_6 gas but also for C_4FN – CO_2 and C_5FK – Dry Air mixtures with presence of protrusion defect inside a real size HVDC GIS.

2 TEST SETUP & PROCEDURES

2.1 INSULATING GAS

The choice of insulating gases is explained in [8] and is summarized in Table 1. The gas mixture composition and pressure are chosen to have the same theoretical dielectric strength as SF_6 at 500 kPa. It is calculated using the density normalized critical electric field [8].

Table 1. Investigated gases and the corresponding gas pressures

Gas	Gas component	Pressure (kPa)
SF_6	SF_6	500
C_5FK – Dry Air mixture	C_5FK – Dry Air 6.6 %	750
	Novec 5110 – C_5FK	50
	Dry Air	700
C_4FN – CO_2 mixture	C_4FN-CO2 10 %	650
	Novec 4710 – C_4FN	65
	CO_2	585

2.2 DEFECT AND TEST SETUP

A needle is on purpose introduced in a real size 320 kV HVDC GIS to simulate the protrusion defect in the equipment. A tungsten needle with 10 mm in length, 0.51 mm in body diameter, and 25 µm in tip radius (Figure 6) is thus fixed on the high voltage conductor of the GIS (Figure 1). The outer radius of the high voltage conductor is 46 mm, the inner radius of the enclosure is 190 mm and the gas volume is about 0.15 m^3 in the test compartment.

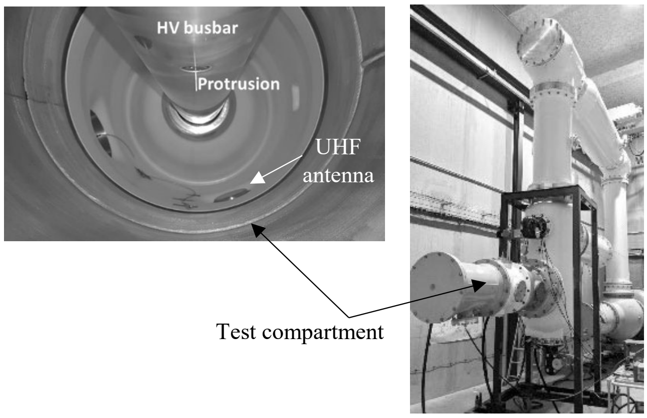

Figure 1. Installation of the defect in the test compartment and test setup for PD long term investigation

Should be noted that the needle is relatively long compared to usual defect size inside apparatus. However, such length facilitates the comparison of PD behavior of SF_6 and SF_6 alternative gases as well as the study of PD behavior over time thanks to the lower PD inception voltages.

To perform the long-term test, a test setup was built to permanently apply DC voltage on the test compartment (Figure 1). The AC voltage generated by AC GIS voltage transformer is converted to DC voltage thanks to a diode rectifier. The test compartment is filled with different gases at different pressures as indicated in Table 1. Humidity absorber is also installed in the test compartment to ensure dry gas as in real equipment.

2.3 MEASURING SYSTEMS

The test circuit for conventional PD measurement is depicted in Figure 2. A coupling capacitor of 1 nF is connected to the test compartment and thanks to the measuring impedance Z_m, Omicron CLP542, the PD conventional measurement, compliant with the IEC 60270 [11], is performed.

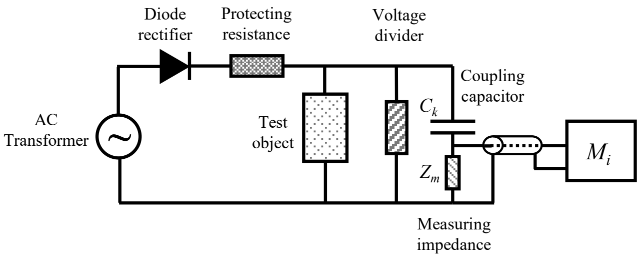

Figure 2. Circuit for DC PD conventional measurement

In addition to the conventional measurement, PD measurement with UHF antenna is also performed as it is the most used technique for the monitoring of AC GIS [12]. The PD wave obtained with UHF antenna is amplified using 28 dB pre-amplifier (R&K LA120-0S 100 MHz – 3200 MHz) before recording with a 500MHz Tektronix DPO5054 oscilloscope. The UHF antenna is installed close to the protrusion defect in the same test compartment as illustrated in Figure 1.

2.4 MEASUREMENT PROCEDURE

Before the test, the PD conventional measuring system was calibrated and the sensivitity check of the UHF measuring system was done. The conventional system was calibrated according to IEC 60270 using an Omicron CAL 542 calibrator. Charge calibration was of 10 pC. On the other hand, a pulse generator UPG 620 is used to verify the sensitivity of UHF PD measurement system according to [12]. The background noise level of the voltage obtained by UHF antenna is also recorded. It should be noted that the maximum noise level is about 0.5 pC at the tested voltage, a filter at 0.5 pC is applied for apparent charge.

To perform long-term PD investigation, a constant voltage of +/-150 kV DC is applied to the test compartment which is 50 % higher than the Partial Discharge Inception Voltage (PDIV). For each test configuration (gas mixture, gas pressure, and voltage polarity) PD measurements were carried out at least once per day for 15 minutes during at least one week.

3 RESULTS

3.1 OBSERVATIONS

An example of a PD measurement with the conventional system and the UHF system is reported in Figure 3 for SF_6 after 7 days at -150 kV DC. Figure 3a points out that the PD generated by the protrusion defect is regular and the apparent charge is almost constant during each recording time meaning 15 minutes, as already observed in [8]. In the UHF measurement (Figure 3b), one can note that the partial discharge can be detected simultaneously with conventional measurement. However, this is not always the case, especially when the PD amplitude is low (about 2 pC – 3 pC) [13]. With low PD apparent charge, the generated electromagnetic wave is very small, it is thus difficult to be picked-up by the UHF system. However when UHF antenna picks up the PD signal, the UHF data can be used as well as the data from the conventional measurement for PD analysis and defect recognition [14].

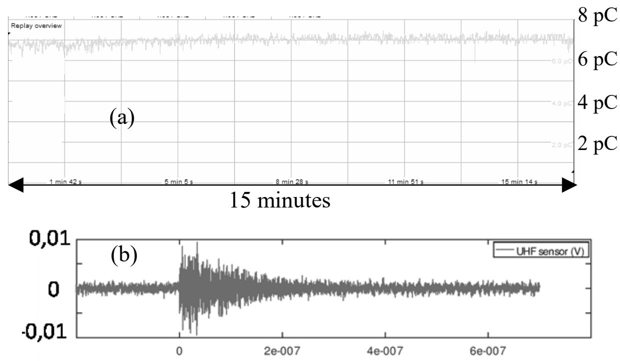

Figure 3. Example of a signal recorded by the conventional measurement during 15 minutes (a) and the same signal recorded with UHF measurement (b) in negative polarity with SF_6 gas.

As the aim of this paper is to investigate the PD long-term behavior of protrusion defect in DC voltage, the UHF measurements are used just as additional information to conventional measurement. Therefore, to simplify the presentation of the results, only results from conventional PD measurements are presented hereafter and the apparent charges are given in absolute values.

3.2 PD EVOLUTION DEPENDING ON THE GAS

Figure 4 shows the evolution of PD apparent charge and PD repetition rate as function of time for SF_6, C_4FN – CO_2, and C_5FK – Dry Air mixtures in both positive and negative polarity at 150 kV DC.

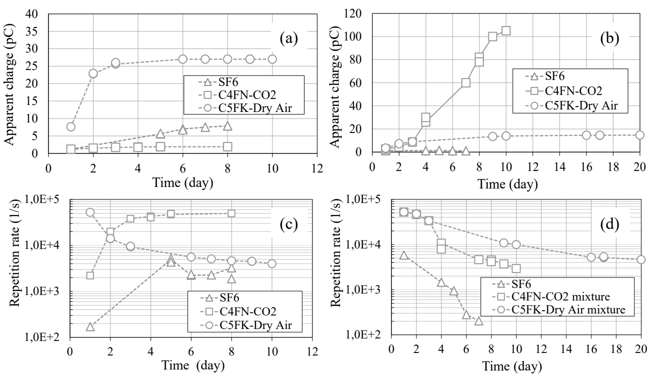

Figure 4. PD Evolution as function of voltage application time for SF_6, C_4FN-CO_2 and C_5FK-Dry Air. (a, b) PD apparent charge and (c, d) PD repetition rate; (a, c) Negative polarity and (b, d) Positive polarity

For SF_6, as illustrated in Figure 4a and 4b, the PD apparent charge is higher in negative polarity. This observation is in accordance with the results presented in [8]. Moreover, PD amplitude increases with the voltage application time in negative polarity while it remains constant in positive polarity. Concerning the PD repetition rate, it increases before reaching a stabilized value in negative polarity while it decreases in positive polarity (Figure 4c and 4d).

Concerning the investigated SF_6 alternative gases, namely

C_4FN – CO_2 mixture and C_5FK – Dry Air mixture, like SF_6, the PD apparent charge and the PD repetition rate change over time. The PD apparent charge increases generally with the voltage application time. The increase is relatively quick for the first days, and it seems to reach a stabilization value after a certain time. The stabilization time varies between the studied gases and depends on the polarity of the applied voltage. As illustrated in Figure 4a and 4b, for C_5FK – Dry air mixture, the stabilization time is 3 days and 10 days for the negative positive polarity and positive polarity respectively. This time is about 3 days and 8 days in negative polarity for C_4FN-CO_2 mixture and SF_6 respectively.

On the other hand, the tested alternative gases present higher PD repetition rate with respect to SF_6 (Figure 4c and d), in accordance with [8][15]. The repetition rate always decreases for all gases in positive polarity. In negative polarity, it increases for SF_6 and for the C_4FN – CO_2 mixture while it decreases for the C_5FK – Dry air mixture. It is worth underlining that the PD repetition rate stabilizes when the PD apparent charge stabilizes.

4 DISCUSSIONS

4.1 EVOLUTION OF PD APPARENT CHARGE

One of the explanations that could be given for the evolution of PD behavior as function of time is the change of gas composition close to the needle tip due to PD activities. Indeed, the gas close to needle tip is subjected to the energy released by PD and is decomposed [16], creating by-products. This change of the gas composition can then lead to a change of PD behavior. To verify this hypothesis, after 10 days of PD long-term test in C_4FN-CO_2 mixture, the voltage has been interrupted during some days before voltage reapplication (Figure 5). If the change of PD behavior is caused by the change of gas composition close to the needle tip, the gas composition will come back to the initial state and thus the initial PD behavior should be observed. However, the PD amplitude remains always the same before and after voltage interruption (Figure 5a). Moreover, the same PD behavior was also observed after recovering all gas inside the test compartment and refilling with new gas (Figure 5b). This observation suggests that the evolution of the PD behavior is not due to the change of gas properties or gas compositions due to PD activities in DC voltage but more likely by geometric modification of the needle itself.

Indeed, to confirm this, photos of the tungsten protrusion are taken before and after each PD long-term test. They are presented in Figure 6, Figure 7, and Figure 8 for the needle before long-term test, after negative polarity for different gases, and after positive polarity for different gases respectively.

Comparing the needle after the test in negative polarity, as pointed out in Figure 7, one can note some differences as a function of the gas. Indeed, the needle after the test in SF_6 presents erosion and material deposition, see zoom in Figure 7a. A material deposition is also observed in C_4FN – CO_2 mixture but in another position, see Figure 7c. For the needle after the test in C_5FK – Dry Air mixture there is no evidence of material deposition but the point is eroded, see zoom in Figure 7b. On the other hand, in positive polarity, after the long term test there is no evidence of material deposition but the points are eroded and a ring scorch mark are visible at the needle termination, see zoom in Figure 8a and b for C_5FK – Dry Air and C_4FN – CO_2 mixtures respectively. Investigation with IRTF spectroscopy have been conducted to identify the nature of the deposited material but unfortunately, due to the 3D geometry it was not possible to conclude. It should however be underlined that the tip radius is increased after the PD long-term test for all investigated gases, it increases from 25 µm at initial state to a value of about 40 µm – 50 µm after the PD long-term investigation.

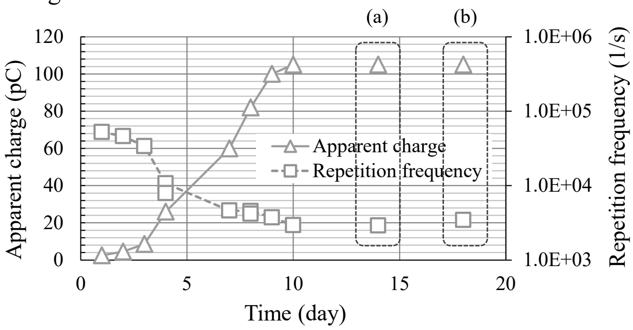

Figure 5. PD amplitude and repetition rate variation for the 10 % C_4FN-CO2 mixture in positive polarity. a) the voltage is reapplied after four days without voltage applications, b) the gas is recovered and refilled before applying again the voltage.

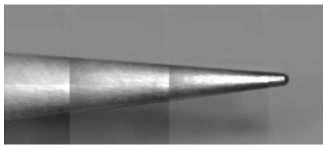

Figure 6. Photo of protrusion defect before PD long-term test.

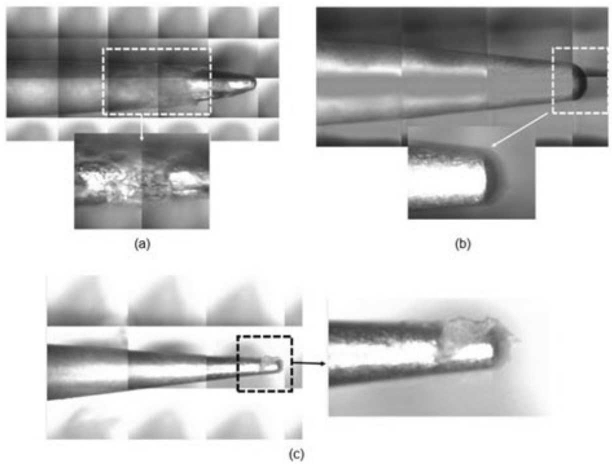

Figure 7. Protrusion defect after PD long-term test in negative polarity for different gases. (a) SF_6, (b) C_5FK-Dry Air, and (c) C_4FN-CO_2.

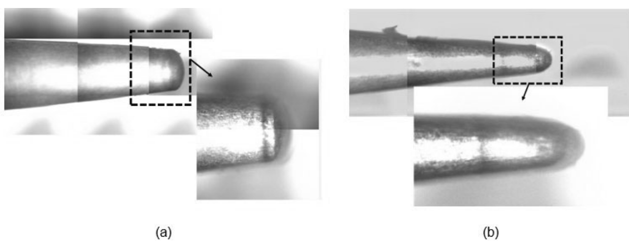

Figure 8. Protrusion defect after PD long-term test in positive polarity for different gases. (a) C_5FK-Dry Air and (b) C_4FN-CO_2.

It is well-known that the partial discharge characteristics of a protrusion depend strongly on its geometry, namely its tip radius, meaning electric field on the needle tip rather than the background electric field. Indeed, sharp protrusion creates very high electrical fields, easily generates electron avalanche and PD activities start easier than in the rounded protrusion. Moreover, the PD behavior depends not only on the absolute value of the electric field but also the ionization region, namely active zone, where the avalanche phenomena happened. In this zone, the ionization coefficient α is higher than the attachment coefficient η, meaning the effective ionization coefficient α_{eff} is higher than zero. During PD activities, the creation of electron takes place in this active volume. For the same defect, voltage polarity and gas nature, the PD apparent charge increases with the applied voltage as presented in [8], it is directly related to the increase of active volume with the increase of voltage. Indeed, the number of generated electrons depends on the active volume: the higher the active volume, the higher the generated electrons and then the higher PD apparent charge.

Although the protrusion needle is made of tungsten material, as presented above, its tip radius has been changed and increased after the PD long term test. It might be due to the electrochemical etching of the material in strong electric field areas. In this case, for the same applied voltage, the active volume with protrusion defect might depend also on the tip radius as illustrated in Figure 9. Higher tip radius can lead to higher active volume and then higher PD apparent charge.

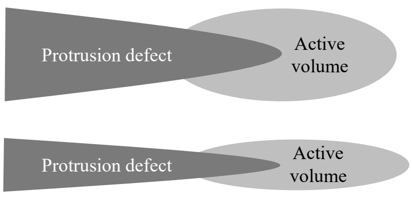

Figure 9. Active volume in function of protrusion tip radius.

To confirm the observed phenomena and to verify the hypothesis above, simulations were performed in 3D coaxial geometry with 46 mm in outer radius of high voltage conductor and 190mm in inner radius of enclosure respectively. The needle with tip radius of 25 µm is exceeded the high voltage conductor of 10 mm. The voltage of -150 kV is applied on the high voltage conductor, the electric field and the active volume where $\alpha_{eff} \geq 0$ are then computed using electrostatic calculation without space charge distortion during PD activities.

The simulated geometry, the electric fields and the active volume are presented in Figure 10. It is observed that the electric field is strongly intensified on the protrusion tip. In this case, a maximum electric field of 450 kV/mm appears on the protrusion tip, while the electric field on the high voltage conductor is only 2.3 kV/mm without the protrusion.

As the tip radius was observed as a changing parameter with time, simulations were then performed for different tip radii. One should underline that the protrusion length exceeding the high voltage conductor decreases when the tip radius increases as the protrusion tip is etched by electrochemical reactions during PD activities. This fact is also considered in the simulation. The active volume where $\alpha_{eff} \geq 0$ is then computed as a function of the tip radius and is presented in Figure 11 for SF_6 gas as an example. It is observed that the active volume changes with the evolution of tip radius. The active volume increases with the increases of tip radius and reaches its maximum value at a tip radius of 40 µm – 50 µm before the decrease when the tip radius continues to increase. As pointed out in Figure 7 and Figure 8, the tip radius at the end of the long-term PD tests is bigger than at the beginning for all the investigated gases: about 50 µm compared to 25 µm. According to Figure 11, the tip radius of 40 µm – 50 µm corresponds to the maximum value of the active volume. As the active volume relates to the PD apparent charge, it might explain the increase of this later with time during PD long-term test.

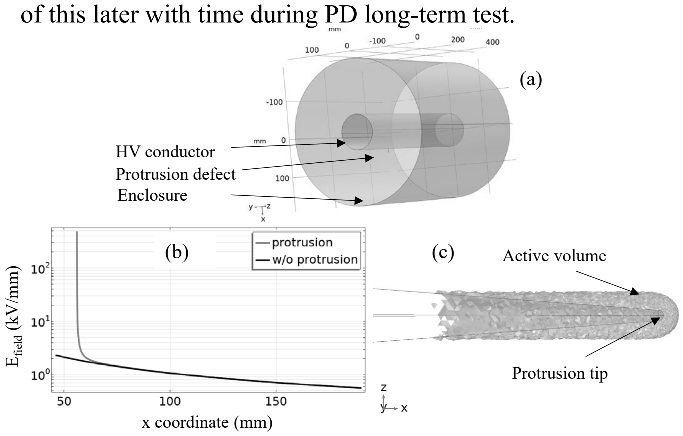

Figure 10. Simulated geometry with a protrusion of 10 mm of length and 25µm of tip radius (a), electric fields along radius with and without protrusion (b), protrusion, and active volume (c).

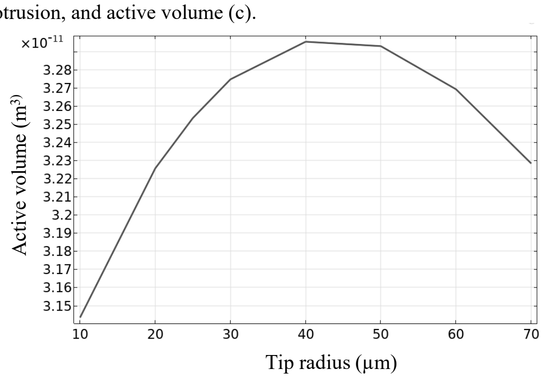

Figure 11. Active volume in function of protrusion tip radius for SF_6 gas.

It should be noted that the active volume presented in Figure 11 is issued from calculation without space charge contribution. Nevertheless, the electric field close to the needle tip is strongly distorted by space charge generated during PD activities. The active volume, the behavior of space charges including electron, negative and positives ions strongly depend on the applied polarity and on the gas nature. These dependences might explain different evolutions of PD apparent charge in function of polarity and gas natures. It is therefore possible to illustrate a qualitive relation between the calculated active volume and PD apparent charge but it is very difficult to establish a quantitative relation.

The erosion of tip radius with time can be estimated by assuming that there is a constant rate of volume reduction of the protrusion. As presented in [17], the dependence of tip radius with time can be expressed by the following equation

$$r_t = C.\sqrt[3]{t} \quad (1)$$

Where r_t is the tip radius (µm), C is a constant ($\mu m/\sqrt[3]{h}$) which depends on the test condition and protrusion material, t is the time (h). According to the experimental data where the tip radius changes from 25 µm initially to about 40 µm – 50 µm after 8 days of test, the constant C is then estimated to be in the range of 2.6 ($\mu m/\sqrt[3]{h}$) and 4.4 ($\mu m/\sqrt[3]{h}$) which is a little smaller than the value presented in [17] (5.7 ($\mu m/\sqrt[3]{h}$)). The difference can be explained by the applied voltage and the insulating nature: DC and gas in this work while AC and liquid in [17]. The tip radius evolution over time can be then illustrated in Figure 12. It points out that the rate of increase of tip radius is very high for the first days, and it becomes smaller the following days of PD activities. This evolution of the tip radius can then explain the evolution of PD apparent charge observed during the PD long term investigation.

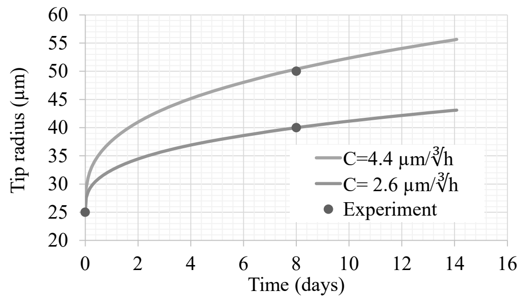

Figure 12. Model for tip radius evolution over time.

Concerning PD repetition rate, the global tendency is the decrease of this latter with time except the cases of C_4FN-CO_2 mixture and SF_6 in negative polarity. The decrease of PD repetition rate with time can also be explained by the increase of tip radius [18]. Indeed, the electric field is very sensitive to the tip radius. When the tip radius increases, the electric field decreases very quickly. In this case, the generation of the first electron for avalanche phenomena is more difficult and it can lead to the decrease of PD repetition rate with time. In cases of C_4FN-CO_2 mixture and SF_6 in negative polarity, the PD repetition rate increases with time. It might be related to the apparition of material deposition on the protrusion defect (Figure 7a and 7c). In this case, the PD source might not only be the protrusion tip but also the material deposition.

4.2 DEFECT PATTERN EVOLUTION

In AC systems, defect recognition by PD measurement can be done thanks to the identification of different defect patterns. The most used technique is the Phase Resolved Partial Discharge analysis (PRPD) where the measured PD signals are synchronized with the zero crossings of the applied voltage. In this case, defect patterns of different defects are distinguishable. However, in DC systems, the defect recognition is more challenging to achieve as there is no phase information. The PRPD pattern is thus non-applicable in a DC system. Different strategies were proposed in the literature in order to distinguish different defects using the Pulse Sequence Analysis (PSA) method [4][6] or by statistical calculation combined with artificial intelligence [19].

Concerning the graphic PSA method, it can give direct visuals for users during a partial discharge measurement. In a conventional measurement, there are two main parameters for each PD event: the time of occurrence t_i, and the apparent charge amplitude q_i. From these two main parameters, different combinations can be used to represent PD signals namely NoDi* plots such as $q_i(\Delta t_i)$, $\Delta q_i(\Delta t_i)$, $\Delta q_{i+1}(\Delta q_i)$, $\Delta t_{i+1}(\Delta t_i)$ …[4][5]. However, Madhar *et al.* points out that the NoDi* plots might have some difficulties to distinguish partial discharge activities with very close physical phenomena like corona discharge and surface discharge [20]. To overcome this problem and to enhance PD diagnostic, the product of Δq_i and Δt_i in function of Δq_i or Δt_i is then proposed to evaluate namely 'Weighted PSA' [20].

In addition to the proposed DC PSA plots cited above, more PSA plots which are the combination of the product $q_i.\Delta t_i$ or by the ratio $q_i/\Delta t_i$ and Δt_i might be interesting. Indeed, the PD apparent charge and the time between PDs are usually physically linked: high apparent charge and low repetition rate or low apparent charge and high repetition rate as illustrated in Figure 4. This proposal might be useful to obtain the fingerprint of each defect. This section presents some examples of the evolution with time of two PSA plots $\Delta q_{i+1}(\Delta q_i)$ and $q_i/\Delta t_i(\Delta t_i)$ of a protrusion defect.

Figure 13, Figure 14 and Figure 15 show the PSA plots of a protrusion defect at different times for SF_6, C_5FK- Dry air and C_4FN-CO_2 respectively. At the initial state, these plots are different for the different investigated gases. This observation is in accordance with the results presented in [5] especially for $\Delta q_{i+1}(\Delta q_i)$ plots. Moreover, the PSA plots of C_4FN-CO_2 mixture and C_5FK-Dry Air mixture are quite close to the one obtained with pure CO_2 and Air respectively [5]. It means that the buffer gas is the main contributor to the PD patterns as the concentration of C_4FN and C_5FK in the mixture is quite low: maximum 10 %.

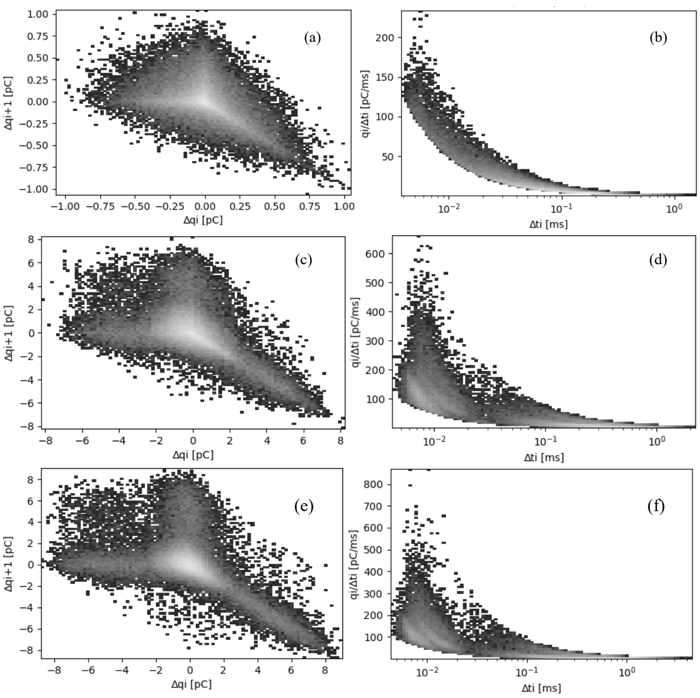

Figure 13. PSA plots of SF6 gas in function of time at – 150 kV DC. (a, b): initial state, (c, d) 5 days and (e, f) 8 days. (a, c, e) $\Delta q_{i+1}(\Delta q_i)$ and (b, d, f) $q_i/\Delta t_i(\Delta t_i)$

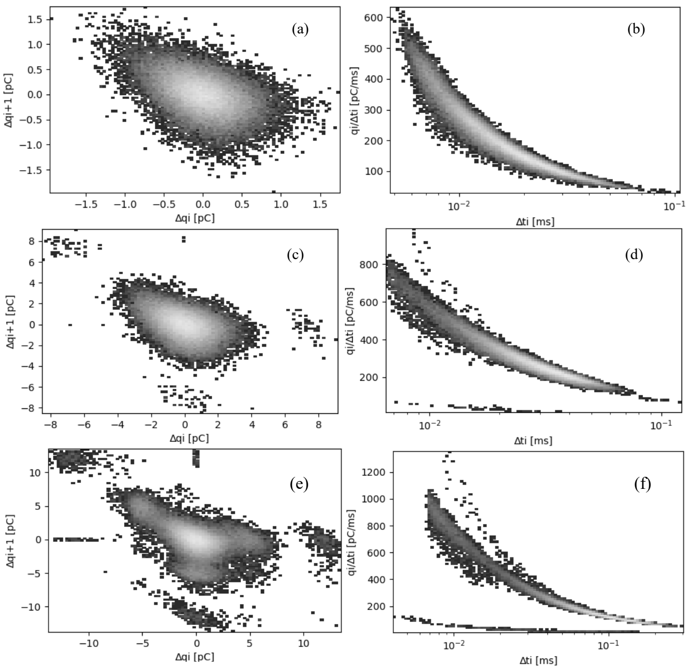

Figure 14. PSA plots of C5FK-Dry Air gas in function of time at + 150 kV DC. (a, b): initial state, (c, d) 3 days and (e, f) 8 days. (a, c, e) $\Delta q_{i+1}(\Delta q_i)$ and (b, d, f) $q_i/\Delta t_i(\Delta t_i)$

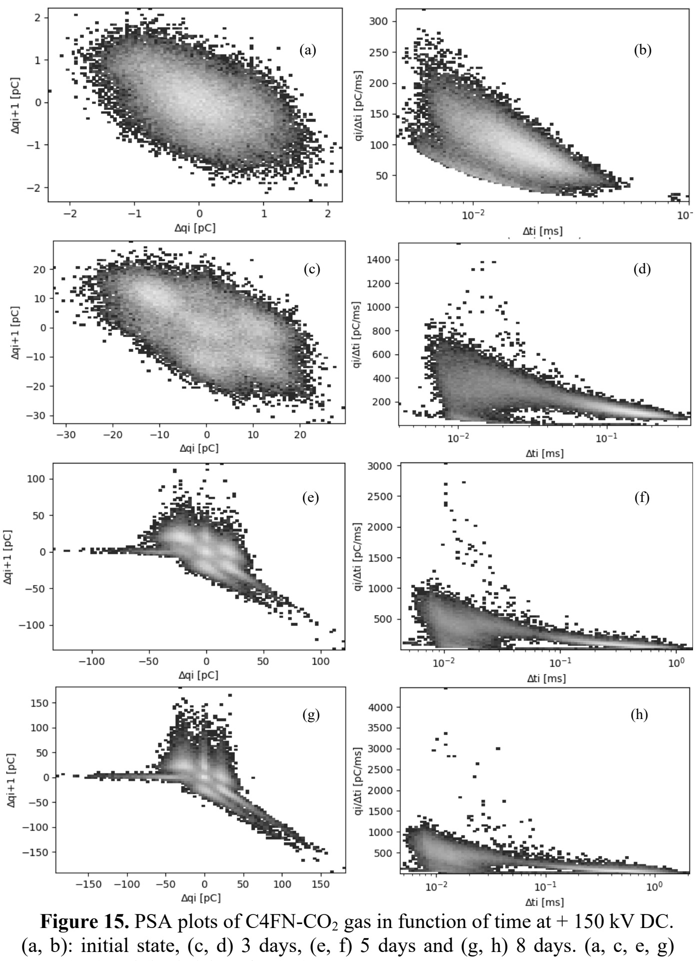

Figure 15. PSA plots of C4FN-CO_2 gas in function of time at + 150 kV DC. (a, b): initial state, (c, d) 3 days, (e, f) 5 days and (g, h) 8 days. (a, c, e, g) $\Delta q_{i+1}(\Delta q_i)$ and (b, d, f, h) $q_i/\Delta t_i(\Delta t_i)$

With time, as the PD apparent charge and the PD repetition rate change, the defect patterns are changing in term of values and in term of pattern shapes. The evolution is progressive and can be seen clearly in Figure 13, Figure 14 and Figure 15. Moreover, the modification of PD pattern is more significant for the C_4FN – CO_2 and C_5FK – Dry Air mixtures than that of SF_6. Indeed, while the shape of PSA plots of SF_6 after 8 days of test (Figure 13e and 13f) remains quite close to the one at the initial state (Figure 13a and 13b), the shape of PSA plots of C_4FN – CO_2 and C_5FK – Dry Air mixtures after some days of test are completely different compared to the one obtained at the initial stage (Figure 14 and Figure 15). This evolution might be challenging for the defect recognition by human expert or by computing tools. If the human expert or computing tools are trained to recognize defects only by PSA plots from short-term PD investigations, the recognition task will be much more difficult or not possible with the evolution of defects if the corresponding PSA plots are not used in the training process. In this case, only PSA plots might not be enough to recognize different defects. The introduction of statistical parameters combined with automatic classification tools becomes more interesting as illustrated in [21]. In any case, these evolutions over time need to be considered in developing PD monitoring and diagnostic tools for HVDC GIS.

5 CONCLUSIONS

This paper presents the long-term PD behavior of a protrusion defect in real size HVDC GIS with different gases including SF_6, C_4FN – CO_2 10% mixture, and C_5FK – Dry Air 6.6% mixture. It is shown that the PD apparent charge and PD repetition rate change over time. In general, the PD apparent charge increases and the PD repetition rate decreases with the increasing of the DC voltage application time. The change of PD behavior has been demonstrated to be directly linked with the increase of protrusion tip radius due to electrochemical etching phenomena caused by PD activities. Therefore no direct correlation between the apparent charge and the defect size/criticality exist. Moreover, protrusion in real application consists, most likely, of weaker materials than the used tungsten needle, then, it is expected that PD in real HVDC application caused by protrusion will behave differently over time. Furthermore, the Pulse Sequence Analysis plots are presented for all investigated gases depending on the voltage application time. It is observed that the PSA plots also changes with the voltage application time. In this case, the defect recognition task becomes challenging as the database is usually established only with short-time PD tests. The PSA characteristics from long-term voltage application need to be studied and considered for training human experts or in automatic defect recognition tools.

ACKNOWLEDGMENT

The work was funded by Horizon 2020 PROMOTioN (Progress on Meshed HVDC Offshore Transmission Networks) project under Grant Agreement No. 691714 and by the French government under the frame of "Investissements d'avenir", No.ANE-ITE-002-01.

REFERENCES

[1] B. De Clercq *et al.,* "Towards a governance model for the European electricity transmission network in 2050," *E-Highway 2050 milestone D5.1*

[2] C. M. Franck, A. Chachereau and J. Pachin, “SF_6 free gas insulated switchgear: Current status and future trends,” *IEEE Electr. Insul. Mag.*, vol 37, no. 1, 2021

[3] SC A3 Workshop, Recent development and interrupting performance with SF_6 alternative gases, *CIGRE*, 2017

[4] A. Pirker and U. Schichler, “Partial discharge measurement at DC voltage – Evaluation and characterization by NoDi* pattern,” *IEEE Trans. Dielec. Electr. Insul.*, vol. 25, no. 3, 2018.

[5] A. Pirker and U. Schichler, “Partial discharges of defects in different insulating gases: N2, CO2, Dry air and SF6,” *IEEE Int. Conf. Prop. Appl. Dielectr. Mat. (ICPADM),* 2018

[6] E. Ouss, L. Zavattoni, A. Beroual, A. Girodet and P. Vinson*,* “Measurement and analysis of partial discharge in HVDC gas insulated substations,” *Cigre Sci. Eng.*, vol. 11, pp. 62-69, 2018.

[7] T. Götz, H. Kirchner and K. Backhaus, “Partial discharge behavior of a protrusion in Gas Insulated Systems under DC voltage stress,” *Energies*, vol. 13, pp. 3102, 2020.

[8] C. Toig, T. Vu-Cong, F. Jacquier and A. Girodet, “Partial discharge behavior of protrusion on high voltage conductor in GIS/GIL under high voltage direct current: comparison of SF6 and SF6 alternative gases”, *IEEE Trans. Dielectr. Electr. Insul.*, vol. 27, pp. 140-147, 2020

[9] G. Wang, W-H. Kim, G-S. Kil, S-W Kim and J-R. Jung*,* “Green gas for grid as an eco-friendly alternative insulation gas to SF6: from the perspective of partial discharge under AC,” *Appl. Sci.*, vol. 9, pp. 651, 2019.

[10] Dielectric testing of gas insulated HVDC systems, *CIGRE Technical Brochure 842 JWG D1/B3.57*, 2021

[11] High voltage test techniques - Partial discharge measurements, IEC standard 60270:2000, 2015-11-27

[12] UHF partial discharge detection system for GIS: Application guide for sensitivity verification, *CIGRE Technical Brochure 654 WG D1.25*, 2016.

[13] C. Toigo *et al.*, “Measurement and behaviour of partial discharge for SF_6 substitute gases in HVDC GIS/GIL,” *CIGRE Paris,* 2020

[14] T. Vu-Cong, M. Dalstein and C. Toigo, F. Jacquier and A. Girodet, “Partial discharge measurement in DC GIS : comparison between conventional and UHF methods,” *Conf. Electr. Insul. Dielect. Phenom. (CEIDP),* 2021

[15] D15.8, “Report on long term monitoring of DC GIS in presence of defects”, *WP15 PROMOTioN Project Deliverable*, 2020

[16] P. Simka, C. B. Doiron, S. Scheel and A. Di-Gianni, “Decomposition of alternative gaseous insulation under partial discharge,” *ISH*, 2019

[17] T.Grav, “Mechanism governing the occurrence of partial discharges in insulation liquids,”, *NTNU MsC thesis*, 2013

[18] Y. Zheng, L. Wang, D. Wang and S. Jia, “Numerical study of the needle tip radius on the characteristics of Trichel pulses in negative corona discharges,” *Phys. Plas.*, vol. 24, 063515, 2017

[19] N. Morette, L. C. Castro Heredia, T. Ditchi, A. Rodrigo Mor and Y. Oussar, “Partial discharges and noise classification undr HVDC using unsupervised and semi-supervised learning,” *Int. J. Elec. Power*, vol. 121, 2020

[20] S. A. Madhar, P. Mraz, A. Rodrigo Mor and R. Ross, “Empirical analysis of partial discharge data and innovative visualization tools for defect identification under DC stress,” Int. J. Elec. Power, vol. 123, 2020

[21] M. Dalstein *et al.*, “Partial discharge recognition tool for MV/HV DC equipment,” *Int. Conf. Dielect. (ICD),* 2022

Cong-Thanh Vu was born in Vietnam, in 1986. He received the MSc degree in 2010 and Ph.D. degree in electrical engineering in 2013 from the University of Grenoble, France. He joined SuperGrid Insitute since 2013 to work on the design insulator for HVDC GIS/GIL. His main research interests include HVDC insulating materials, discharge phenomena including insulating system diagnostics, electric field simulation and insulation design of high voltage apparatus.

Caterina Toigo was born in Italy, in 1991. She received the BSc degree in 2013 and the MSc degree in 2016 in electrical engineering from the University of Padova, Italy. She joined SuperGrid Institute since 2017 to study the application of SF_6 alternative gases on HV apparatus, especially GIS. Her main research interests include SF_6 alternative gases dielectric characterization, HVDC equipment, discharge phenomena and electric field simulations.

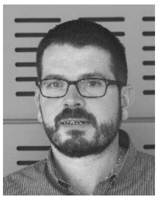

Frank Jacquier was born in France, in 1976. He received the MSc degree in mechanical systems engineering from the University of Technology Troyes, France, in 2000. He joined ALSTOM in 2003, as research engineer. In 2012 he was in charge of Generator Circuit Breaker research group. In 2014, in addition he took the head of the GIS research group. Since 2018, he joined SuperGrid Institute as Technology Department Manager in charge of GIS HVDC development.

Alain Girodet was graduated from Ecole Nationale des Arts et Metiers in 1981. He joined ALSTOM in 1982 as an engineer in the Air-blast Circuit Breaker Research Group. In 1987 he was in charge of the Material and Technology Laboratory of HV Technical Department. In 1992 He took the head of the GIS Research Group to move in 2002 as the manager of the High Voltage Technology and Material Research Department. Since 2014 he is responsible as Program Director of research on AC/DC equipment in SuperGrid Institute. He is also involved as an expert in different CIGRE D1 working groups related to Material and Emerging test techniques.

M**aximilian Nikolaus Tuczek** was born in Frankfurt am Main, Germany, in 1982. He received the Dipl.-Ing. degree in 2008 and Dr.-Ing. degree in 2015 from Technische Universität Darmstadt, Germany. He Joined ABB Deutschland in the GIS Quality Department in 2014. Since 2017 he is in the Asset Management of TenneT TSO GmbH responsible for GIS onshore and offshore in Germany. He was and is involved in several CIGRE and IEC working groups.

Armando Rodrigo Mor is an Industrial Engineer from Universitat Politècnica de València, in Valencia, Spain, with a Ph.D. degree from this university in Electrical Engineering. In Spain, he joined and later led the High Voltage Laboratory and the Plasma Arc Laboratory of the Instituto de Tecnología Eléctrica in Valencia. From 2013 until 2020 he was an Assistant Professor in the Electrical Sustainable Energy Department at Delft University of Technology, in Delft, Netherlands, appointed as head of the High Voltage Team in 2019, and Associate Professor in 2021. Since 2021 he is with Universitat Politècnica de València and the Instituto de Tecnología Eléctrica. His research interests include high voltage testing, monitoring and diagnostic, sensors for high voltage applications, high voltage technology, space charge measurements and HVDC.

Uwe Riechert (M’13) is a senior principal engineer and project manager for gas-insulated HVDC and HVAC substations and circuit-breaker at Hitachi Energy Switzerland in Zurich. He finished the studies in electrical engineering at the Dresden Technical University (TUD) in 1994 and received the Ph.D. at the TUD on the topic of polymeric insulated HVDC cables in 2001. Since 1999 he is with ABB Switzerland, later Hitachi ABB Power Grids and today Hitachi Energy Switzerland. He conducted several product development projects in the field of gas-insulated switchgear, high current systems, UHV substations and HVDC gas-insulated systems. From 2017 to 2020 he was allowed to lead the HVDC GIS work package within the European PROMOTioN project. Uwe Riechert is a member of national committees in Germany and Switzerland (DKE and CES) and member or convener of different CIGRE and IEC working groups. He is convener of the CIGRE advisory group AG D1.02: High voltage and current testing and diagnostic and of the IEC 17C WG 42: DC gas-insulated switchgear assemblies.